Richards, F. M., & Wyckoff, H. W. (1971) *Enzymes, 3rd Ed. 4*, 647–806.
Roberts, G. C. R., Dennis, E. A. Meadows, D. H., Cohen, J. S., & Jardetzky, O. (1969) *Proc. Natl. Acad. Sci. U.S.A. 62*, 1151–1158.
Schowen, R. L. (1978) in *Transition States of Biochemical Processes* (Gandour, R. D., & Schowen, R. L., Eds.) pp 77–114, Plenum Press, New York.
Shapiro, R., & Klein, R. S. (1966) *Biochemistry 5*, 2358–2362.
Swain, C. G., & Brown, J. F., Jr. (1952) *J. Am. Chem. Soc. 74*, 2534–2537.
Swain, C. G., DiMilo, A. J., & Gordner, J. P. (1958) *J. Am. Chem. Soc. 80*, 5983–5988.
Westheimer, F. H. (1968) *Acc. Chem. Res. 1*, 70–78.
Wolfenden, R. (1973) *Acc. Chem. Res. 5*, 10–18.

Energetics of Ribonuclease A Catalysis. 3. Temperature Dependence of the Hydrolysis of Cytidine Cyclic 2′,3′-Phosphate†

Maurice R. Eftink* and Rodney L. Biltonen

ABSTRACT: Studies of the temperature dependence of the steady-state kinetics of the ribonuclease A catalyzed hydrolysis of cytidine cyclic 2′,3′-phosphate at pH 5.0 are reported. Contributions to the temperature dependence of the apparent Michaelis–Menten parameters from temperature-sensitive protonic equilibria (primarily the coupled protonation/deprotonation of the active-site histidine residues) were incuded in our analysis. The data were interpreted by employing a transition-state approach. By comparing the temperature dependence of the rate constant for the nonenzymatic hydrolysis of the substrate with the temperature dependence of the enzyme-catalyzed reaction, we obtained values for the enthalpy change, entropy change, and heat capacity change for the interaction of the reaction transition state with the enzyme. These thermodynamic quantities were then interpreted by comparison with corresponding values for the binding of cytidine 2′- and 3′-phosphate to the enzyme. A model is presented for the enzyme–transition-state interaction involving the favorable transfer of a proton from the transition state to a histidine residue at the active site and the formation of hydrogen bonds and van der Waals contacts between the pyrimidine ring of the transition state and the enzyme's binding pocket. These elementary interactions are consistent with the determined values of the enthalpy change and entropy change, as well as earlier reported ionic strength and solvent isotope dependence studies. The Gibbs energy contributions from these elementary interactions have also been estimated, giving a sum approximately equal to the experimentally determined value for the stabilization energy of the enzyme–transition-state complex. The model thus provides an explanation for the magnitude of the $\sim 10^{10}$-fold rate enhancement achieved by this enzyme.

Interpretation of the temperature dependence of the kinetics of enzyme-catalyzed reactions has proven to be a difficult task. The activation enthalpy ($\Delta H^{\ddagger}$)[1] and activation entropy ($\Delta S^{\ddagger}$) that are determined for such reactions will reflect not only the electronic and geometric changes taking place within the substrate molecule(s) as it (they) form(s) the transition state but also any concomitant changes in the state of the enzyme, including changes in solvation. The activation parameters for several enzymes have been tabulated (Laidler, 1955; Laidler & Peterman, 1979; Lumry, 1959), and it has been noted that there is a general tendency for the enzyme to lower $\Delta H^{\ddagger}$. Other studies have focused on the observation of curved Arrhenius plots for certain enzyme-catayzed reactions (Massey et al., 1966; Dixon & Webb, 1964; Levy et al., 1959). Such curvature can be attributed to the existence of a thermally induced reversible change in the conformation of the protein (Massey et al., 1966) or to the existence of consecutive reaction steps with different individual activation enthalpies (Kitskiakowsky & Lumry, 1949). Frequently the enzymes displaying anomalous Arrhenius plots happen to be membrane associated (Thilo et al., 1977; Linden et al., 1973; Raison, 1973).

In this paper, we offer an alternative strategy for interpreting activation parameters in terms of the transition-state theory of enzyme catalysis. As will be discussed below, one can convert the information in $\Delta H^{\ddagger}$ (and $\Delta S^{\ddagger}$) to an enthalpy change (and entropy change) for the association of the transition state with the enzyme. One may then attempt to interpret these equilibrium thermodynamic parameters in terms of the elementary interactions responsible for the stabilization

† From the Department of Chemistry, The University of Mississippi, University, Mississippi 38677 (M.R.E.), and the Departments of Biochemistry and Pharmacology, University of Virginia School of Medicine, Charlottesville, Virginia 22903 (R.L.B.). *Received January 24, 1983.* Supported by National Science Foundation Grants PCM 75-23245, PCM 79-23031, and PCM 80-03645 and National Institutes of Health Postdoctoral Fellowship 1F 32 GM 0 594201 (to M.R.E.). A preliminary report of this work has appeared (Eftink & Biltonen, 1978).

[1] Abbreviations: cCMP, cytidine cyclic 2′,3′-phosphate; 3′-CMP, cytidine 3′-phosphate; 2′-CMP, cytidine 2′-phosphate; k_c, apparent first-order rate constant for the enzyme-catalyzed reaction ($k_c = V_m/[E]$ where V_m is the maximum velocity); $k_{\bar{c}}$, pH-independent value of k_c as defined in Eftink & Biltonen (1983a); $\Delta H^{\ddagger}_{k_{\bar{c}}}$ and $\Delta S^{\ddagger}_{k_{\bar{c}}}$, activation enthalpy and entropy, respectively, for $k_{\bar{c}}$; k_E, first-order rate constant for an enzyme-catalyzed reaction (equivalent to k_c); k_{NE}, rate constant for the nonenzymatic conversion of the substrate to the product; k_{Im}, rate constant for the imidazole-catalyzed conversion of the substrate to the product; K_m, apparent Michaelis constant for the enzyme, equal to K_S^{-1} in the present studies with ribonuclease and cCMP; $K_{\bar{m}}$, pH-independent value of K_m as defined in Eftink & Biltonen (1983a); $\Delta H^{\circ}_{K_{\bar{m}}}$, $\Delta S^{\circ}_{K_{\bar{m}}}$, and $\Delta C^{\circ}_{p,K_{\bar{m}}}$, enthalpy change, entropy change, and heat capacity change, respectively, for the interaction between cCMP and ribonuclease; K_{TS}, ΔH°_{TS}, ΔS°_{TS}, and $\Delta C^{\circ}_{p,TS}$, association constant, enthalpy change, entropy change, and heat capacity change, respectively, for the interaction of the reaction transition state with the enzyme; RNase A, bovine pancreatic ribonuclease A.

0006-2960/83/0422-5140$01.50/0

of the transition state at the active site of the enzyme. This may be facilitated by comparing the enthalpy change (and entropy change) for the association of the transition state with the same thermodynamic parameters for the association of other ligands and transition-state analogues to the enzyme.

We will use such an approach in studying the temperature dependence of the ribonuclease A (RNase A) catalyzed hydrolysis of cytidine cyclic 2′,3′-phosphate (cCMP). In the preceding papers (Eftink & Biltonen, 1983a,b), we have reported extensive studies of the steady-state kinetics of this enzyme and studies of the nonenzymatic hydrolysis of cCMP, including the activation parameters for the latter reaction. These studies provide necessary groundwork for the present analysis. Thorough studies of the thermodynamics of the binding of 2′- and 3′-CMP to RNase A have also been performed (Flogel & Biltonen, 1975a,b; Eftink et al., 1983). Since the dianionic form of these is believed to closely resemble the pentacoordinated intermediate formed during the enzymatic hydrolysis of cCMP, the thermodynamic information for these ligands (2′- and 3′-CMP) will be of value in interpreting the enthalpy and entropy changes for the association of the transition state with the enzyme.

In this paper, we will also propose a mechanism for RNase A catalysis that allows an explanation for the magnitude of the rate enhancement of the enzymatic reaction.

Theory

According to the transition-state theory of enzyme catalysis, the rate constants for the enzymatic reaction, k_E, and an appropriate nonenzymatic reference reaction, k_{NE}, are related to the association constant of the transition state, K_{TS}, to the enzyme by the following equation [see Wolfenden (1972) and Lienhard (1973) for details]:

$$k_E/k_{NE} = K_{TS}/K_S \tag{1}$$

For systems in which K_M, the Michaelis constant, is equal to K_S^{-1}, the relationship can be rewritten as eq 2 (also substituting

$$(k_c/K_m)(1/k_{NE}) = K_{TS} \tag{2}$$

k_c for k_E). Note that k_c/K_m is the apparent second-order rate constant for the enzyme-catalyzed reaction.

From the above equations, it is a simple matter to write the following relationships (eq 3a,b) between the activation en-

$$\Delta H^{\ddagger}_E - \Delta H^{\ddagger}_{NE} + \Delta H^{\circ}_S = \Delta H^{\circ}_{TS} \tag{3a}$$

$$\Delta H^{\ddagger}_{k_c/K_m} - \Delta H^{\ddagger}_{NE} = \Delta H^{\circ}_{TS} \tag{3b}$$

thalpies for the enzymatic ($\Delta H^{\ddagger}_E$) and nonenzymatic ($\Delta H^{\ddagger}_{NE}$) reactions and the enthalpy changes for the binding of the substrate (ΔH°_S) and transition state (ΔH°_{TS}). A similar relationship can be written for the activation entropies and the entropy changes (eq 4a,b). (Note that $\Delta H^{\ddagger}_{k_c/K_m}$ and $\Delta S^{\ddagger}_{k_c/K_m}$

$$\Delta S^{\ddagger}_E - \Delta S^{\ddagger}_{NE} + \Delta S^{\circ}_S = \Delta S^{\circ}_{TS} \tag{4a}$$

$$\Delta S^{\ddagger}_{k_c/K_m} - \Delta S^{\ddagger}_{NE} = \Delta S^{\circ}_{TS} \tag{4b}$$

are the activation parameters for the second-order rate constant for the enzyme-catalyzed reaction.) Therefore, by experimentally determining $\Delta H^{\ddagger}_{NE}$, $\Delta H^{\ddagger}_{NE}$, and ΔH°_S (or $\Delta H^{\ddagger}_{k_c/K_m}$), one can determine ΔH°_{TS} (and likewise ΔS°_{TS}).

If there is an induced change in the structure of the enzyme or a change in the structure of the transition state (i.e., if the enzyme-bound transition state is different from the nonenzymatic transition state) upon the interaction between the two, this may be reflected by a change in the heat capacity, $\Delta C^{\circ}_{p,TS}$, for the binding of the transition state to the enzyme. Consider

Scheme I

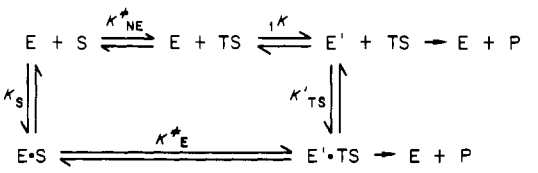

Scheme II

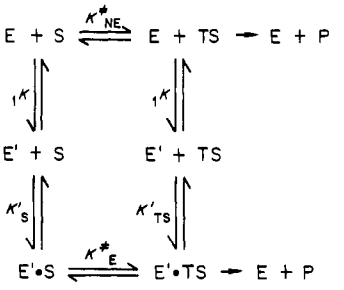

Scheme I in which the transition state, TS, binds preferentially to some altered structural state of the enzyme, E′. The binding of the transition state will induce the E → E′ transition in the protein ($_1K$ = [E′]/[E]), and the enthalpy change for the binding of the transition state will be temperature dependent (eq 6), giving rise to a ΔC_p as indicated by eq 7.[2] In such

$$\frac{K_S K^{\ddagger}_E}{K^{\ddagger}_{NE}} = \frac{k_c}{K_m k_{NE}} = K'_{TS1}K/(1 + {}_1K) \tag{5}$$

$$\Delta H^{\ddagger}_{k_c/K_m} - \Delta H^{\ddagger}_{NE} = \Delta H^{\circ}_{TS}{}' + {}_1\Delta H^{\circ} - \frac{{}_1K_1\Delta H^{\circ}}{1 + {}_1K} = \Delta H^{\circ}_{TS}(\text{app}) \tag{6}$$

$$\frac{d[\Delta H^{\circ}_{TS}(\text{app})]}{dT} = \frac{-{}_1\Delta H^{\circ 2}{}_1K}{RT^2(1 + {}_1K)^2} = \Delta C^{\circ}_{p,TS} \tag{7}$$

a case, the $K^{\ddagger}_E$ step would include a dynamic involvement of the protein (conformational change) in forming the transition state at the enzyme's active site. Such equations also apply if there is some change in the structure of the transition state (in which case $_1K$ would represent the equilibrium constant for such a transition).

One might also expect the binding of the substrate to induce a change in the conformation of the enzyme and thus produce a change in heat capacity, $\Delta C_{p,S}$. Such a possibility is illustrated by Scheme II and eq 8–11, where we consider the

$$\frac{k_c}{k_{NE}}\frac{K'_{S1}K}{1 + {}_1K} = \frac{K'_{TS1}K}{1 + {}_1K} \tag{8}$$

$$1/K_m(\text{app}) = \frac{K'_{S1}K}{1 + {}_1K} \tag{9}$$

$$\Delta H^{\circ}_{K_m}(\text{app}) = \Delta H^{\circ}_S{}' + {}_1\Delta H^{\circ} - \frac{{}_1K_1\Delta H^{\circ}}{1 + {}_1K} \tag{10}$$

$$\Delta C^{\circ}_{p,S} = \frac{-{}_1\Delta H^{\circ 2}{}_1K}{RT^2(1 + {}_1K)^2} \tag{11}$$

induced E → E′ transition to be the same for both substrate

[2] We assume in deriving the expressions for the heat capacity changes that the induced conformational change is the only contributing factor; that is, there is no significant temperature dependence of ΔH°_{TS} or ΔH°_S. Also, we have assumed the induced conformational change to be a two-state transition. A more realistic description might be an induced multistate transition [see Eftink et al. (1983)].

Scheme III

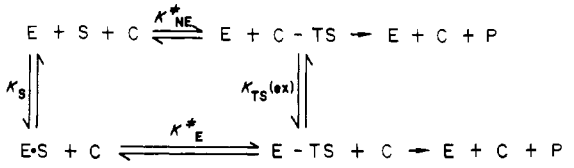

and transition-state binding. The enthalpy change and heat capacity change for the binding of the substrate will be given by eq 10 and 11, which are similar to eq 6 and 7 for the binding of the transition state.

The above relationships are based on the comparison of the enzyme-catalyzed reaction with some noncatalyzed reaction. Another useful approach is to compare the enzymatic reaction with a reaction catalyzed by a small molecule analogue of an active-site catalytic residue of the enzyme. In the particular case investigated here, we will compare the imidazole- (general base) catalyzed hydrolysis of cCMP to the enzyme-catalyzed reaction (where general base catalysis by an active-site histidine residue is operative). A diagram for such an analysis is shown in Scheme III (Jencks, 1975). In comparing the activation enthalpies for the two reactions, one obtains $\Delta H^{\circ}_{TS}(ex)$, the enthalpy change for the exchange of the transition state between the catalyst, C, in solution and the enzyme's active site. (In eq 12–14, the nonenzymatic reaction refers to the small molecule catalyzed reaction.)

$$\frac{k_c}{K_m k_{NE}} = K_{TS}(ex) \tag{12}$$

$$\Delta H^{\ddagger}_{k_c/K_m} - \Delta H^{\ddagger}_{NE} = \Delta H^{\circ}_{TS}(ex) \tag{13}$$

$$\Delta S^{\ddagger}_{k_c/K_m} - \Delta S^{\ddagger}_{NE} = \Delta S^{\circ}_{TS}(ex) \tag{14}$$

The above-described strategy for analyzing the temperature dependence of an enzyme-catalyzed reaction can also be extended to study the dependence on other experimental variables such as ionic strength, pH, pressure, solvent isotope, or chemical substituent. From studies of the dependence of k_{NE} and k_c/K_m on these experimental variables, x, one can determine the functional dependence of K_{TS} on the variable (i.e., $\delta K_{TS}/\delta x$). Again, by comparing $\delta K_{TS}/\delta x$ with the dependence of the association constant of a transition-state analogue ($\delta K_{analogue}/\delta x$) or the substrate ($\delta K_S/\delta x$) on the variable x, one can gain insight concerning the elementary interactions between the enzyme and the transition state.

Experimental Procedures

Materials. Phosphate-free RNase A and cCMP were obtained from Sigma Chemical Co. and were used without further purification. Deionized water was used to prepare the 0.05 M (ionic strength = 0.2 M with NaCl) acetate buffer.

Kinetic Studies. The steady-state kinetics of the RNase A catalyzed hydrolysis of cCMP were determined by use of the spectroscopic method of Crook et al. (1960) using a Cary 14 spectrophotometer equipped with an extended-scale slide wire. Briefly, 750 μL of a substrate solution, preequilibrated at the experimental temperature, was added to a temperature-jacketed cuvette. After a few minutes were allowed for further temperature equilibration and for the recording of a base line, enzyme was added with a 10-μL Hamilton syringe. After the solution was mixed for about 20 s, the increase in absorbance at 295 nm was recorded for the next 10 min or until the absorbance became greater than 0.2. Temperature was controlled by a Lauda K2R water bath, and the temperature inside the jacketed cuvette was measured with a thermister probe.

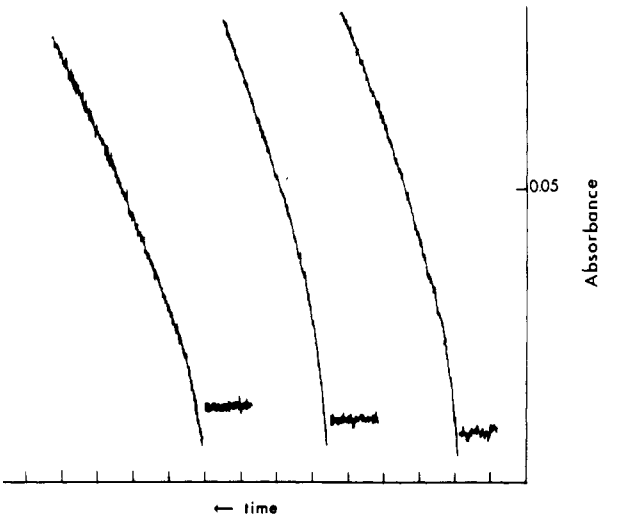

FIGURE 1: Typical progress curves for the RNase A catalyzed hydrolysis of cCMP. The above curves were obtained at low temperature (8.5 °C) where the nonlinearity of the progress curves is most pronounced. The two curves to the right are for an initial substrate concentration of 2×10^{-3} M; the curve to the left is for a concentration of 1×10^{-3} M. Due to the obvious difficulty in determining initial velocities for these curves, the data were analyzed by using an integrated rate equation as described under Experimental Procedures of this paper and of a preceding paper (Eftink & Biltonen, 1983a). The time axis is in divisions of 160 s.

At temperatures below 17 °C, a stream of air was directed at the cuvette in order to prevent condensation.

The progress curves obtained for this system are quite curved, particularly at low temperatures, due to product inhibition. Typical progress curves are shown in Figure 1. The product 3′-CMP binds approximately 10-fold more strongly than does the substrate at pH 5.0 (Eftink & Biltonen, 1983a). At 5% reaction progress, the apparent initial velocity will be about 20% smaller than the true initial velocity at $[S]_0 = K_m$. Therefore, it is mandatory to include product inhibition in the analysis of the kinetics of RNase catalysis. We have accomplished this by making use of the integrated form of the Michaelis–Menten equation including product inhibition. Details of this analysis are given in Eftink & Biltonen (1983a). The K_p values for 3′-CMP needed for this analysis were determined independently as follows. A dissociation constant for 3′-CMP of 7.2×10^{-5} M^{-1} was determined at 25 °C, ionic strength 0.2 M, pH 5.0, by using flow microcalorimetry (Eftink & Biltonen, 1980a). From this value and the ΔH° of −9 kcal/mol for 3′-CMP binding at this pH, the K_p values at other temperatures were calculated.

Kinetic measurements were performed as a function of cCMP concentration from 2×10^{-3} to 2×10^{-4} M in order to determine V_m and K_m. As can be noted from Table I, the highest $[S]_0$ in each experiment was greater than the determined K_m value. Progress curves at each substrate concentration were performed in duplicate or triplicate.

The change in extinction coefficient, $\Delta\epsilon_{295}$, for the hydrolysis of cCMP to 3′-CMP was found to be temperature dependent at pH 5.0. Figure 2 shows the manner in which $\Delta\epsilon$ varies with temperature. We have measured $\Delta\epsilon$ both by allowing the reaction to go to completion and by directly comparing the absorption spectra of cCMP with those of 3′-CMP at different temperatures.

All pH measurements were made with a Radiometer 4b pH meter. The concentration of protein solutions was determined by using an extinction coefficient of 9800 M^{-1} cm^{-1} (Tanford et al., 1955).

Table I: Temperature Dependence of the Michaelis–Menten Parameters for the RNase A Catalyzed Hydrolysis of cCMP[a]

T (K)	K_m ($\times 10^4$ M)	k_c (s^{-1})	k_c/K_m (M^{-1} s^{-1})	K_p[b] ($\times 10^5$ M)	$\Delta\epsilon_{295}$ (M^{-1} cm^{-1})
281	6.2	0.78	1260	3.2	1030
284.5	5.7	0.86	1500	3.7	970
292	5.8	1.23	2120	5.5	820
298	5.4	1.40	2570	7.2	760
306	8.6	2.28	2650	10.7	705
308.5	8.2	2.20	2670	11.7	675
312.5	9.6	2.50	2600	14.2	640
318	16.8	4.06	2400	18.0	610
321.5[c]	22.5	4.65	2060	22.2	585

[a] Ionic strength, 0.2 M. [b] K_p values determined by assuming a value of 7.2×10^{-5} M at 25 °C and a $\Delta H°$ of 3′-CMP binding of −9.0 kcal/mol at pH 5.0. [c] Highest substrate concentration, 3×10^{-3} M.

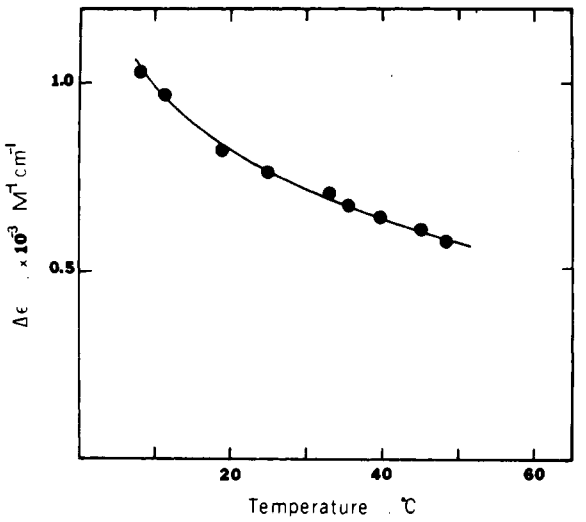

FIGURE 2: Temperature dependence of $\Delta\epsilon$ at 295 nm for the cCMP → 3′-CMP reaction at pH 5.0, 0.2 M ionic strength (due primarily to the temperature dependence of the absorbance of 3′-CMP).

Results

In Table I are listed the rate constant, k_c, Michaelis constant, K_m, and second-order rate constant, k_c/K_m, for the RNase A catalyzed hydolysis of cCMP at pH 5.0, ionic strength 0.2 M, and at temperatures from 8 to 45 °C. Figure 3 illustrates the Arrhenius and van't Hoff plots of these data. The Arrhenius plot for k_c is linear over the entire $1/T$ range. On the other hand, plots of log (k_c/K_m) and $-\log K_m$ vs. $1/T$ show a clear downward curvature. Note that while the k_c and K_m values are subject to correlation in errors, the ratio k_c/K_m will have less error.

Matheson & Scheraga (1979) have also published data on the temperature dependence of the hydrolysis of cCMP. They reported a nonlinear Arrhenius plot for the initial velocity, v_i, from 10 to 50 °C. Most of their data were taken at a single substrate concentration, 0.63 mM. They argued that their initial velocity measurements were proportional to k_c and that the temperature dependence of v_i therefore reflected the temperature dependence of k_c. They justified this argument by performing three measurements at higher substrate concentration.

Our data are clearly in disagreement with those of Matheson & Scheraga (1979). In our studies, each k_c value was obtained by extrapolation of initial velocity measurements made at at least six different (and duplicated) substrate concentrations. Also, our highest $[S]_0$ was always greater than the determined

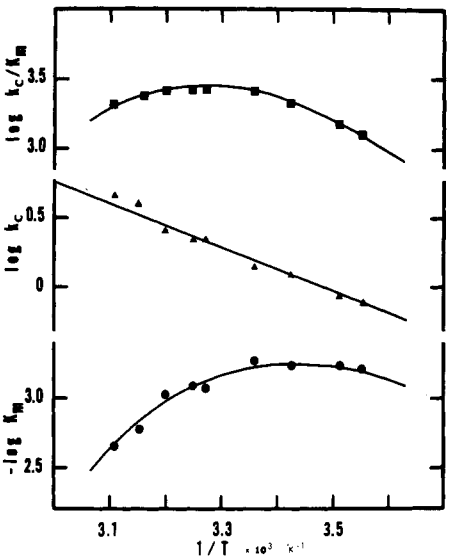

FIGURE 3: van't Hoff plot for the apparent K_m and Arrhenius plots for the apparent first-order and second-order rate constants for the RNase A catalyzed hydrolysis of cCMP at pH 5.0.

K_m, a condition needed to assure a reliable determination of k_c. There has been no report of the K_m for cCMP at pH 5.0 and ionic strength 0.1 M, the conditions used by Matheson and Scheraga. However, by interpolation of our data taken at ionic strengths of 0.05 and 0.2 M (Eftink & Biltonen, 1983a), one can see that Matheson and Scheraga's experiments were performed at a $[S]_0$ approximately equal to K_m. Also, Matheson and Scheraga apparently made no attempt to correct for product inhibition, which is more severe at low temperature than at high temperature, and they did not mention inclusion of the temperature dependence of $\Delta\epsilon$ in their analyses. Since $\Delta\epsilon_{295}$ decreases with temperature (see Figure 2), if this decrease is not realized, the apparent velocities at high temperatures will be underestimated. These several reasons can explain the discrepancy between the two sets of data; we feel that the present data are more reliable due to our use of higher $[S]_0$ and our consideration of product inhibition (by use of an integrated Michaelis–Menten equation) and the temperature dependence of $\Delta\epsilon$.

Our studies were performed at pH 5.0 to enable a correction to be made for the pH dependence of the enzymatic reaction. It has previously been demonstrated by ourselves (Eftink & Biltonen, 1983a) and others (Herries et al., 1962; del Rosario & Hammes, 1969) that the pH dependence of k_c, K_m, and k_c/K_m can be described by a model involving two ionizable histidine residues (His-12 and -119) at the enzyme's active site along with one other ionizing group, tentatively assigned as the 3-imino group of the cytosine ring. The respective equations for the pH dependence of the kinetic parameters are given as eq 3 and 4 in the first paper in this series (Eftink & Biltonen, 1983a), along with the fitted values of K_a and K_b (the dissociation constants of His-12 and -119, respectively, on the free enzyme), $K_{a,s}$ and $K_{b,s}$ (the dissociation constants of the same histidine residues in the enzyme–substrate complex), and k_c and K_m [the pH-independent rate constant and Michaelis constant, respectively; see Table II, solution set 2 in Eftink & Biltonen (1983a)].

From the Arrhenius plot of k_c(app), an apparent activation enthalpy of 7.5 kcal/mol is found, in agreement with the value found by Cheung & Abrash (1964) for the catalyzed hydrolysis of cUMP under similar conditions. The temperature dependence of k_c(app) will, however, include a contribution from the temperature dependence of the protonation/depro-

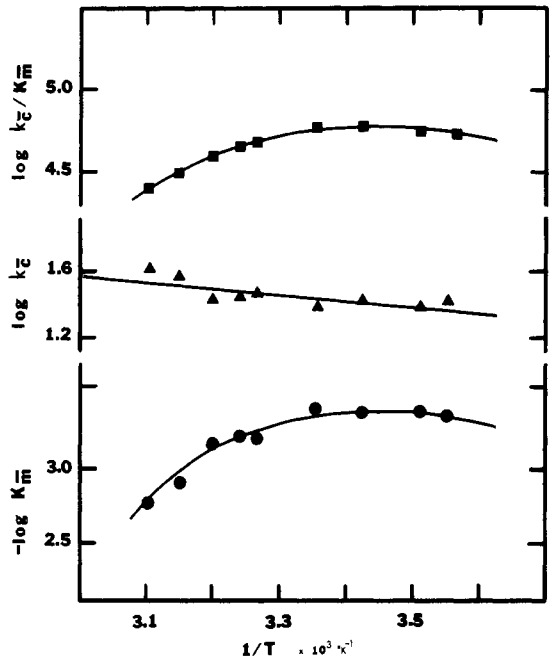

FIGURE 4: van't Hoff plot for the pH-independent $K_{\bar{m}}$ and Arrhenius plots for the pH-independent first-order and apparent second-order rate constants for the RNase A catalyzed hydrolysis of cCMP. $K_{\bar{m}}$, k_c, and $k_c/K_{\bar{m}}$ were calculated from pH-dependent values as described in the text by using the pK_a, pK_b, $pK_{a,s}$, and $pK_{b,s}$ values given in Eftink & Biltonen (1983a) and heats of protonation of −6.5 kcal/mol for both His-12 and His-119 and −4.4 kcal/mol for group "C", tentatively assigned as the 3-imino group of cCMP.

tonation of the active-site histidine residues in the enzyme–substrate complex. At pH 5.0, the pH dependence of k_c(app) can be approximated by [see eq 3 of Eftink & Biltonen (1983a)]

$$k_c(\text{app}) = \frac{k_c}{[H^+]/K_{b,s}} \qquad (15)$$

The temperature-induced deprotonation of His-119 will thus contribute largely to the apparent $\Delta H^{\ddagger}_{k_c}$. A value of $pK_{b,s}$ = 6.25 has been assigned by our steady-state enzyme kinetic studies. The heat of protonation of His-119 in the enzyme–substrate complex has not been directly measured. However, since studies by Flogel & Biltonen (1975a) have shown that the heat of ionization of the histidine residues of RNase A does not change significantly from a value of −6.5 kcal/mol upon the binding of 3′-CMP, we choose this value in our present analysis.

Using these values for $K_{b,s}$ and $\Delta H^{\circ}_{b,s}$, we can correct the temperature dependence of the apparent k_c for the contribution due to the ionization of His-119. When this is done, we obtain the Arrhenius plot in Figure 4 which is an Arrhenius plot for k_c. The plot remains linear, and the activation enthalpy for k_c is found to be 1.0 kcal/mol.

Also, the temperature dependence of the apparent K_m at pH 5.0 will include a very small contribution from the temperature-dependent protonation/deprotonation of the active-site histidine residues and the 3-imino group of the substrate. The proton dissociation constant and heat of protonation of these groups have been determined by NMR (Markley, 1975; Patel et al., 1975) and calorimetric studies (Flogel & Biltonen, 1975a). In Figure 4 is shown the resultant temperature dependence of $K_{\bar{m}}$ that can be calculated from the temperature dependence of K_m that is analogous to eq 3 and 4 in Eftink & Biltonen (1983a)]. As can be seen, the van't Hoff plot for $K_{\bar{m}}$ remains downward curving even after these corrections. The curvature indicates that there is a negative heat capacity change, $\Delta C^{\circ}_{p,K_{\bar{m}}}$, associated with the interaction of the substrate with the enzyme. The following equation can describe an association process having a significant heat capacity change:

$$-\ln K_{\bar{m}} = \frac{-\Delta H^{\circ}_0}{RT} + \frac{\Delta S^{\circ}_0 - \Delta C^{\circ}_{p,K_{\bar{m}}}}{R} + \frac{\Delta C^{\circ}_{p,K_{\bar{m}}} \ln T}{R} \qquad (16)$$

where ΔH°_0 and ΔS°_0 are the enthalpy and entropy change at $T = 0$, respectively. The apparent enthalpy change at other temperatures is $\Delta H^{\circ} = \Delta H^{\circ}_0 + T\Delta C^{\circ}_{p,K_{\bar{m}}}$. The solid line in Figure 4 illustrates the fit of the above equation to the data for $\Delta C^{\circ}_{p,K_{\bar{m}}} = -150$ cal/(mol·deg). The $\Delta H^{\circ}_{K_{\bar{m}}}$ at 25 °C is found to be −2.0 kcal/mol.

Finally, the contribution to the temperature dependence of k_c/K_m(app) at pH 5.0 from the protonation/deprotonation of the histidine residues and the 4-amino group of the substrate can be accounted for in a similar fashion. Shown in Figure 4 is the Arrhenius plot for $k_c/K_{\bar{m}}$. As with the van't Hoff plot for $K_{\bar{m}}$, this Arrhenius plot is downward curving. On analyzing the data according to an equation analogous to eq 16, we obtain a value of −150 cal/(mol·deg) for the activation heat capacity change, $\Delta C^{\ddagger}_{p,k_c^-/K_m^-}$, for the second-order enzyme-catalyzed reaction. The $\Delta H^{\ddagger}_{k_c^-/K_m^-}$ value at 25 °C is calculated to be −1.1 kcal/mol.

Discussion

In this section, we will first discuss the temperature dependence of the k_c and $K_{\bar{m}}$ values for the RNase A catalyzed hydrolysis of cCMP by focusing on the activation thermodynamics of these Michaelis–Menten parameters. We will then offer an interpretation of these data in terms of the transition-state approach presented under Theory. Finally, we will discuss the energetics of the RNase A catalyzed reaction in an attempt to explain the magnitude of the rate enhancement achieved by this enzyme.

In Table II are listed the activation and thermodynamic parameters describing the RNase A catalyzed hydrolysis of cCMP and various nonenzymatic hydrolysis reactions. The thermodynamic parameters for the interaction of the transition state with the enzyme (see section B) are also listed, along with values for the interaction of 2′-CMP and 3′-CMP with RNase A. The latter information is included to provide a basis for comparison of the enthalpy change and entropy change for the binding of the substrate and the transition state to the enzyme. It should be noted that the thermodynamic values for 2′-CMP and 3′-CMP are for the binding of the dianionic form of the nucleotides to the state of the protein having both active-site histidine residues protonated. The $\Delta H^{\ddagger}_{k_c^-}$, $\Delta H^{\circ}_{K_m^-}$, ΔH°_{TS}, and ΔH°_{TS}(ex) values (and respective entropy changes) determined in this study are for the interaction (or reaction) of the substrate or transition state with the state of the enzyme having one histidine protonated and the other unprotonated. This difference in the state of protonation of the enzyme must be kept in mind in the comparisons made below. The standard state for all thermodynamic parameters is unit molarity.

(A) Activation Thermodynamics of the Michaelis–Menten Parameters. The $\Delta H^{\ddagger}_{k_c^-}$ value of 1.0 kcal/mol for the RNase A catalyzed reaction is quite small compared to most reported activation enthalpies for enzymatic reactions. Also, the value is much smaller than that for the various nonenzymatic hydrolysis reactions of cCMP (Eftink & Biltonen, 1983b). The small $\Delta H^{\ddagger}_{k_c^-}$ value indicates that the enthalpy barrier for

Table II: Activation Thermodynamic Values for the Enzymatic and Nonenzymatic Hydrolysis of cCMP[a]

	cCMP → 3′-CMP			
	$\Delta G^{\ddagger}$ (kcal/mol)	$\Delta H^{\ddagger}$ (kcal/mol)	$\Delta S^{\ddagger}$ [cal/(mol·deg)]	$\Delta C^{\ddagger}_p$ [cal/(mol·deg)]
enzymatic				
$k_{\bar{c}}$	15.5 ± 0.1	1.0 ± 0.4	−48.6 ± 1.6	
$k_{\bar{c}}/K_{\bar{m}}$	11.1 ± 0.2	−1.1 ± 0.2	−40.9 ± 1.3	−150 ± 50
nonenzymatic				
H_2O	29.1 ± 0.5	17.0 ± 5.0	−40 ± 18	
OH^-	19.5 ± 0.1	21.0 ± 2.0	5.0 ± 7.0	
imidazole	25.9 ± 0.1	11.0 ± 2.0	−50.0 ± 7.0	
	RNase–Ligand Interaction			
	ΔG° (kcal/mol)	ΔH° (kcal/mol)	ΔS° [cal/(mol·deg)]	ΔC°_p [cal/(mol·deg)]
2′-CMP	−8.4[b] ± 0.1	−6.6 ± 1.0	6.0 ± 3.6	−120 ± 20[c]
3′-CMP	−7.0[b] ± 0.1	−7.1 ± 0.7	0 ± 2.6	−150 ± 20[c]
cCMP ($K_{\bar{m}}$)	−4.5 ± 0.2[d]	−2.0 ± 1.0	8.0 ± 4.0	−150[e]
transition state (K_{TS})	−18.0 ± 0.7	−18.0 ± 5.0	0 ± 19	−150[f]
transition state exchange ($K_{TS,ex}$)	−14.8 ± 0.3	−12.0 ± 2.0	9.4 ± 7.6	−150

[a] Values for 25 °C. All thermodynamic values are for a standard state of 1 M. [b] Refers to the binding of dianionic nucleotide to the state of the protein having both active-site histidines protonated. From Flogel et al. (1975) and references cited therein. [c] The ΔC°_p for 2′-CMP and 3′-CMP binding has been corrected for protonic equilibria contributions as described in Eftink et al. (1983). [d] Refers to the binding of monoanionic cCMP to the state of the protein having one histidine protonated and the other unprotonated. [e] The ΔC°_p for cCMP binding was assumed to be −150 cal/(mol·deg) in order to obtain $\Delta H^{\circ}_{K_{\bar{m}}}$. The data for the temperature dependence of $K_{\bar{m}}$ are consistent with a $\Delta C^{\circ}_{p,K_{\bar{m}}}$ of this magnitude, but data are not of high enough quantity to obtain a nonforced determination of $\Delta C^{\circ}_{p,K_{\bar{m}}}$. [f] This value assumes the heat capacity of activation for the water reaction, $\Delta C^{\ddagger}_{p,w}$, to be zero. Actually, a small, negative $\Delta C^{\ddagger}_{p,w}$ [−30 to −40 cal/(mol·deg)] is expected for k_w from analogy with studies of the hydrolysis of methanesulfonate esters (Barnard & Robertson, 1961), but such a value is still small compared to $\Delta C^{\ddagger}_{p,k_{\bar{c}}/K_{\bar{m}}}$.

formation of the transition state is very low and that overcoming the activation entropy barrier [$\Delta S^{\ddagger}_{k_{\bar{c}}}$ = −48.6 cal/(mol·deg)] actually limits the reaction rate. These activation parameters suggest a situation in which the enzyme, by utilizing various means of assistance, is able to virtually eliminate the enthalpy barrier for forming the transition state. As will be discussed below, these means include the transfer of a proton from the attacking water molecule to one of the active-site histidine residues and an interaction between residues constituting the binding site of enzyme and the pyrimidine ring of the substrate/transition state. The large negative activation entropy suggests that the limiting factor is the coordination in space and time of the attack of the water molecule and the interactions with residues at the enzyme's active site.

The enthalpy change for the association of cCMP with RNase A is −2.0 kcal/mol, and, as indicated by the curvature in Figures 3 and 4, a heat capacity change of −150 cal/(mol·deg) also characterizes this interaction. The $\Delta H^{\circ}_{K_{\bar{m}}}$ is significantly smaller than the value of −7.1 kcal/mol for the enthalpy change for the binding of 3′-CMP to RNase A [see Table II and Flogel et al. (1975)]. In the first paper in this series (Eftink & Biltonen, 1983a), we presented evidence based on the pH dependence of the apparent K_m that cCMP does not bind to RNase A in the same manner as does 3′-CMP. cCMP appears to bind almost entirely through an electrostatic interaction between its phosphate group and the protonated histidine residues of the protein. The molecular basis for the difference in binding is proposed to be due to the fact that the riboside portion of cCMP is rigidly locked in a syn conformation about its glycosidic bond (Lavallee & Coulter, 1973), whereas 3′-CMP readily interconverts between syn and anti forms. Since X-ray diffraction studies (Richards & Wyckoff, 1971) indicate that 3′-nucleotides bind in the anti conformation, this suggests that the pyrimidine ring of cCMP cannot readily interact with the complementary polar groups lining the binding site of the protein. The fact that $\Delta H^{\circ}_{K_{\bar{m}}}$ is less (negative) than that for the binding of 3′-CMP is consistent with this description. The ΔH° of −7 kcal/mol for the binding of 3′-CMP has been interpreted as being due to the formation of hydrogen bonds and van der Waals contacts between the pyrimidine ring of the ligand and the mentioned complementary groups of the binding site (Flogel et al., 1975). If such interactions are not possible with cCMP, $\Delta H^{\circ}_{K_{\bar{m}}}$ would be expected to be smaller (less negative) than that for 3′-CMP.

The $\Delta S^{\circ}_{K_{\bar{m}}}$ for cCMP binding, 8.0 cal/(mol·deg), is slightly larger than that for the binding of 3′-CMP, but approximately the same as that for the binding of 2′-CMP. This is as expected if an electrostatic interaction between cCMP and the enzyme is of primary importance.

The $\Delta C^{\circ}_{p,K_{\bar{m}}}$ of −150 cal/(mol·deg) is also similar to the heat capacity change for the binding of 2′-CMP or 3′-CMP (Eftink & Biltonen, 1980b; Eftink et al., 1983). For the latter ligand, we have considered various possible sources for the negative ΔC°_p and have concluded that the major source is a ligand-induced change in the conformation of the protein. In particular, we have interpreted this conformational change as being a shift in the distribution of structural microstates upon ligand binding (a subtle conformational change). The fact that the ΔC°_p values for the binding of cCMP and the 3′-nucleotide are nearly the same suggests that the substrate induces a similar type of conformational change. If, as discussed above, the riboside portion of cCMP does not interact optimally with the enzyme, then it appears that the interaction between the phosphate group of the substrate (or ligand) and the histidine residues of the protein is primarily responsible for triggering the conformational change. As we will discuss below, a negative heat capacity change is also found for the "binding" of the transition state to the enzyme.

(*B*) *Transition-State Approach: Thermodynamics of the Enzyme–Transition-State Interaction.* By taking the approach described under Theory, one can obtain values for the enthalpy change, ΔH°_{TS}, entropy change, ΔS°_{TS}, and heat capacity change, $\Delta C^{\circ}_{p,TS}$, for the association of the transition state with the enzyme from the activation parameters for the second-order rate constant, $k_{\bar{c}}/K_{\bar{m}}$, and the nonenzymatic "water" reaction[3] (Eftink & Biltonen, 1983b) (see eq 3, 4, and 7).

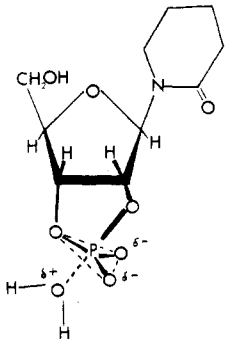

FIGURE 5: Proposed transition state for the cCMP → 3′-CMP reaction.

Values of −18 ± 5 kcal/mol and 0 ± 19 cal/(mol·deg) are found for $\Delta H°_{TS}$ and $\Delta S°_{TS}$, respectively. The large error in the $\Delta H°_{TS}$ and $\Delta S°_{TS}$ values is due to the difficulty in determining the activation enthalpy for the water reaction (Eftink & Biltonen, 1983b). From the heat capacity change of activation for k_t/K_m (and assuming a negligible heat capacity of activation for the water reaction), a value of −150 cal/(mol·deg) can be determined for $\Delta C°_{p,TS}$. Note that in determining $\Delta H°_{TS}$, $\Delta S°_{TS}$, and $\Delta C°_{p,TS}$ we have compared the enzymatic reaction at 0.2 M ionic strength and a temperature range of 10–40 °C to the water reaction at 1.0 M ionic strength and a temperature range of 50–90 °C. It was not feasible to study the enzymatic and nonenzymatic reactions under identical conditions.

The $\Delta H°_{TS}$ value is much larger (negative) than that found for the enthalpy change for the binding of 2′-CMP or 3′-CMP to RNase A. In order to rationalize this difference and also to attempt to interpret the meaning of $\Delta S°_{TS}$ and $\Delta C°_{p,TS}$, we must first propose a model for the transition state of the water reaction and the way in which this transition state interacts with the enzyme. The proposal must be consistent with other information concerning the enzymatic and nonenzymatic reactions as well as allowing the explanation of the magnitude of $\Delta H°_{TS}$, $\Delta S°_{TS}$, and $\Delta C°_{p,TS}$.

We propose the transition state shown in Figure 5, based on the arguments presented in the preceding papers (Eftink & Biltonen, 1983a,b). In the transition state, a partial positive charge is developed on the attacking water molecule and a partial negative charge is developed on an oxygen of the phosphate group. Also, we propose that the pyrimidine ring of the transition state is oriented in an anti-like conformation with respect to the ribose ring. When associated with the enzyme, van der Waals interactions and hydrogen bonds are proposed to form between the pyrimidine ring of the transition state and the complementary groups at the binding site. The twisting of the pyrimidine ring from a syn to an anti conformation would provide a basis for the improved interaction of the enzyme with the transition state, as compared to the substrate. If the interaction between the pyrimidine ring of the transition state and the enzyme is assumed to be optimal, then one would expect a contribution to $\Delta H°_{TS}$ of approximately −7 kcal/mol, the value for the binding of the pyrimidine ring of 3′-CMP.

This leaves approximately −11 kcal/mol of $\Delta H°_{TS}$ to be explained by other interactions. Another such interaction will involve the transfer of a proton from the developing oxonium ion of the transition state to a histidine residue on the protein (i.e., general base catalysis) upon binding. Since the heat of protonation of the active-site histidine residue is approximately −6.5 kcal/mol (Flogel & Biltonen, 1975a), the complete transfer of a proton from the transition state to the histidine residue could account for an additional large contribution to $\Delta H°_{TS}$. The degree to which the proton is transferred to the histidine residue is unknown, but if this transfer is complete, one can readily account for a value of about −13.5 kcal/mol for the binding enthalpy of the transition state shown in Figure 5. Although this value is within the error limits of our determined value of −18 kcal/mol, we suspect that additional exothermic interactions will occur between the transition state and the enzyme. In section C, we will discuss some additional interactions that may be of importance. However, we believe the two above-mentioned interactions, that between the pyrimidine ring and the binding site and the transfer of a proton from the transition state to the active-site histidine residue, are the major elementary interactions to be considered.

The heat capacity change for the binding of the transition state, $\Delta C°_{p,TS}$, is approximately equal to that for the enzyme–3′-CMP interaction and the enzyme–cCMP interaction. As discussed above in relationship to the enzyme–cCMP interaction and under Theory, the fact that similar heat capacity changes are found suggests that a conformational change in the protein accompanies the binding of each of the ligands, including the transition state. Since any induced conformational change will be expensive in terms of the Gibbs energy, the determined association constant for the hypothetical enzyme–transition state interaction must be lower than the intrinsic association constant of the transition state to the optimal conformation of the enzyme (K'_{TS} in Scheme I). "Induced-fit" conformational changes are often found or proposed for protein–ligand and enzyme–substrate interactions; the present study indicates that an induced conformational change can occur as well when one considers the hypothetical binding of a transition state to an enzyme.

The enzymatic reaction can also be compared to the imidazole-catalyzed reaction by using eq 12–14. A $\Delta H°_{TS}$(ex) value of −12 ± 2 kcal/mol is obtained. Since general base catalysis (by imidazole or His-119) is involved in both reactions, the $\Delta H°_{TS}$(ex) will, to a first approximation, reflect interactions between the enzyme and the transition state other than that between His-119 and the pentacoordinated phosphate of the transition state. Again, we expect a contribution of approximately −7 kcal/mol from the binding of the pyrimidine ring of the transition state to the binding pocket. The remaining −5 kcal/mol may be due to some additional interactions. However, it may also be due to the fact that there is a greater degree of proton transfer to His-119 in the enzymatic reaction as compared to the imidazole-catalyzed reaction.

In addition to providing a basis for analyzing the temperature dependence of enzymatic reactions, eq 1 can also be used to analyze ionic strength and solvent isotope studies (see discussion under Theory). From studies of the ionic strength

[3] Note that the rate constant and activation parameters for the "water" reaction were actually obtained by using cUMP rather than cCMP as substrate. An interfering side reaction occurs with cCMP, making it impossible to obtain the kinetic parameters for the water reaction with this substrate. We expect there to be no significant difference between the activation parameters for the water reaction for the two substrates. Also, note that by comparing the enzymatic reaction with the water reaction we are assuming that the enzyme enhances the rate of attack of water rather than hydroxide ion. The presumed general base catalysis by one of the histidine residues of RNase A may actually represent general acid assisted attack of hydroxide ion. However, for this to be the case, the rate of the reaction of the bound substrate with hydroxide ion (when both active-site histidines are protonated) would have to be approximately 10^9 M^{-1} s^{-1}, a value approaching the diffusion-controlled limit. We therefore consider that the enzyme-catalyzed reaction proceeds by the attack of a water molecule.

dependence of k_c/K_m and k_{Im} (where k_{Im} refers to the imidazole-catalyzed reaction), one can determine that the magnitude of K_{TS}(ex) decreases 5-fold as the ionic strength is increased from 0.3 to 1.0 M (Eftink & Biltonen, 1983b). This dependence on ionic strength indicates that there is an electrostatic interaction between the transition state and the enzyme as one would anticipate from the proposed structure of the transition state and the involvement of a protonated His-12 in the enzymatic reaction. Comparing the solvent deuterium isotope effect on both k_c/K_m [i.e., $[k_c/K_m(H_2O)]/[k_c/K_m(D_2O)] = 4.2$] and the rate constant for the imidazole-catalyzed hydrolysis of cCMP [$k_{Im}(H_2O)/k_{Im}(D_2O) = 3.8$], one finds that K_{TS}(ex) does not vary significantly with the solvent isotope. Similarly, no change in K_m for cCMP was found upon substitution of D_2O.

(*C*) *Analysis of the Energetics of RNase A Catalysis and Proposed Mechanisms.* While the dependence of the enzymatic reaction on experimental variables such as temperature, ionic strength, and solvent isotope can be interpreted by using the transition-state approach, the real test of our understanding of the molecular basis of enzyme catalysis lies in our ability to evaluate the Gibbs energy change for the interaction of the transition state with the enzyme ($\Delta G°_{TS} = -RT \ln K_{TS}$). The value that we have determined for $\Delta G°_{TS}$ is -18.0 ± 0.7 kcal/mol. If the Gibbs energy contributions from the various elementary interactions between the transition state and the enzyme can be summed to equal this value of $\Delta G°_{TS}$, then we can confidently say that we understand the basis for the catalytic efficiency of the enzyme. As discussed above, the value of $\Delta H°_{TS}$, along with other information, suggests that the major elementary interactions between the transition state and the enzyme are (a) the pyrimidine ring–binding site interaction and (b) the partial transfer of a proton from the transition state to the active-site histidine residue (His-119). Below we attempt to estimate the Gibbs energy contributions from these elementary interactions to see if they account for the value of −18 kcal/mol.

In order to assess these Gibbs energy contributions, it is necessary that we consider the interactions of fully bonded, activated intermediate species (such as $I^{+,2-}$) rather than

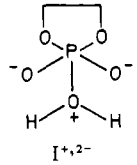

$I^{+,2-}$

partially bonded, true transition-state species (such as that in Figure 5). It is necessary to do this in order to model the above-mentioned elementary interactions. The partially bonded nature of the transition state and the unknown degree of proton transfer in the enzyme–transition-state complex make it difficult to consider the Gibbs energy changes involving these states. A pentacoordinated phosphorus intermediate is believed to form during the hydrolysis of cyclic phosphate esters (Westheimer, 1968). Such an intermediate would be considered to occupy a trough in a free-energy/reaction-coordinate profile following the peak for the transition state [as in Figure 6 of the preceding paper (Eftink & Biltonen, 1983b)], and, invoking the Hammond postulate, the intermediate $I^{+,2-}$ should closely resemble the actual transition state. It should be noted that $I^{+,2-}$ need not be a significantly populated intermediate in the hydrolysis reaction. As discussed in the preceding paper, it is likely that there will be a rapid, intramolecular transfer of a proton from the oxonium group of $I^{+,2-}$ to one of the other phosphate oxygens. This does not deter our use of $I^{+,2-}$ in the following analysis, as $I^{+,2-}$ needs only to be a possible structure that can form during the reaction.

Scheme IV

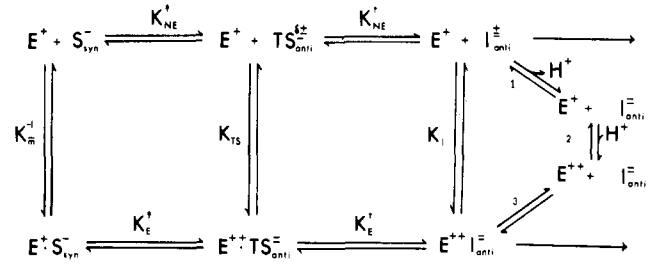

Also, instead of the partially bonded enzyme–transition-state complex, we will focus on the complex between the enzyme and an intermediate in which the proton is fully donated to His-119. To illustrate our ploy, consider Scheme IV which includes these various ground (S), transition (TS), and intermediate (I) states and the thermodynamic steps for their interconversion. $K^{\dagger}_{NE}$ and $K^{\dagger}_{E}$ are the equilibrium constants for the conversion of the transition state to the intermediate for the nonenzymatic and enzymatic reactions, respectively. K_I is the association constant for $I^{+,2-}$ to the monoprotonated state of the enzyme, E^+, to form the complex $E^{2+}I^{2-}$. Included in this binding step is the transfer of a proton to His-119 of the enzyme. In general, the value of K_I will be

$$K_I = K_{TS}\frac{K^{\dagger}_{E}}{K^{\dagger}_{NE}}$$

The value of K_I will be greater than, less than, or equal to the value of K_{TS}, depending on the ratio $K^{\dagger}_{E}/K^{\dagger}_{NE}$. If it is assumed that the ratio $K^{\dagger}_{E}/K^{\dagger}_{NE}$ does not differ too much from unity, then K_I will be approximately equal to K_{TS}. If we can rationalize the magnitude of K_I (or $\Delta G°_I$) in terms of the elementary interactions between $I^{+,2-}$ and the enzyme, this corresponds to a rationalization of the magnitude of K_{TS} (or $\Delta G°_{TS}$).

The association of $I^{+,2-}$ to the enzyme can further be divided into three thermodynamic steps which will enable an estimation of the value of K_I. First, one can consider the transfer of a proton from $I^{+,2-}$ to the active-site histidine residue to proceed in two discrete steps; the dissociation of a proton from $I^{+,2-}$ (step 1) and the protonation of this histidine residue (step 2). One can then consider the association of the resultant dianionic intermediate, I^{2-}, to the state of the enzyme having both histidine residues protonated (step 3).

As we have discussed above and as has been discussed by Flogel et al. (1975), the binding of the dianionic state of 2′-CMP and 3′-CMP to the diprotonated state of RNase A can be used as a model for step 3. The dianionic state of these nucleotides is though to resemble I^{2-} both with respect to the double negative charge on the phosphate groups and with respect to their existence in an anti conformation. Therefore, for both I^{2-} and these nucleotides, the association process (to E^{2+}) should involve van der Waals/hydrogen bonds between the riboside moiety and the binding site and an electrostatic interaction between the protonated histidine residues and the dianionic phosphate group. A value of −8.4 kcal/mol has been determined for the $\Delta G°$ for the binding of 2′-CMP to diprotonated RNase A (Flogel et al., 1975). The $\Delta G°$ for 3′-CMP binding is less negative than that for 2′-CMP by 1.4 kcal/mol, possibly due to the fact that the phosphate group of the latter is located such as to more effectively maximize electrostatic interactions with the active-site histidine residues. Taking the above $\Delta G°$ value for 2′-CMP binding as a model

for step 3, we are left with a Gibbs energy change of −9.6 kcal/mol for the proton-transfer steps.

The ΔG for step 2 (at pH 7) can readily be evaluated from knowledge that the pK_a of His-119 is 6.2 in the free enzyme. This gives a value of 1.1 kcal/mol for step 2.

Thus, a Gibbs energy change of approximately −10.7 kcal/mol must be assigned to the proton dissociation of $I^{+,2-}$ at pH 7. This ΔG value corresponds to the intermediate species having a pK_a of −0.8. If this pK_a is in fact a reasonable one, then the model that we have presented provides an explanation for the forces involved in RNase A catalysis.

The pK_a of an intermediate such as $I^{+,2-}$ cannot be directly measured.[4] We must rely on theory and chemical intuition in order to estimate its value. An approach to predicting the pK_a of $I^{+,2-}$ is to use the empirical relationships of Branch & Calvin (1941). Their method, which predicts the pK_a of compounds by considering the inductive effects of neighboring atoms, has been found to quite accurately predict the pK_a of many compounds. In employing the method of Branch and Calvin for the proton dissociation represented in the following equation, we consider $I^{+,2-}$ to be a derivative of $R\text{–}OH_2^+$, for

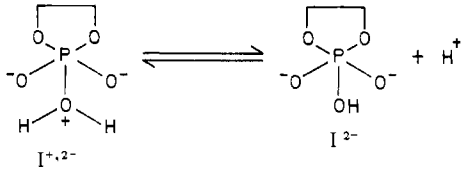

which the pK_a is approximately −2. On including the inductive effect of the neighboring phosphorus, the oxygens, and the two negative charges, we calculate the pK_a of $I^{+,2-}$ to be ~0. As discussed above, a pK_a of the intermediate $I^{+,2-}$ of approximately −0.8 is needed to "explain" the energetics of RNase A catalysis in terms of Scheme IV. The predicted value of ~0 is quite close to this value, particularly when one considers the uncertainties in the method of estimating this pK_a. On summing the Gibbs energy contributions for the binding of $I^{+,2-}$, we obtain $\Delta G°_I$ = −9.6 kcal/mol (step 1) + 1.1 kcal/mol (step 2) − 8.4 kcal/mol (step 3)] = −16.9 kcal/mol. This estimated value of $\Delta G°_I$ approaches the value of $\Delta G°_{TS}$ = −18.0 kcal/mol calculated from our kinetic data (see Table II). We therefore conclude that Scheme IV includes most of the pertinent features needed to explain the catalytic process. The actual rate enhancement (k_c/K_{NE}) for the RNase A catalyzed hydrolysis of cCMP is 7×10^9 (Eftink & Biltonen, 1983b); the above model accounts for a rate enhancement of 1×10^9.

This success in accounting for the energetics of RNase A catalysis is achieved by considering only two major elementary interactions between the enzyme and the transition state/intermediate, those being the transfer of a proton from the attacking water molecule to one of the histidine residues of the enzyme and the interaction between the pyrimidine ring and the binding pocket of the enzyme. It is likely, however, that there are additional features of the enzyme–transition-state interaction that cannot be adequately mimicked by the binding of 2′-CMP. If so, this could provide a basis for an even greater affinity of the transition state/intermediate for the enzyme and could allow further rationalization of the magnitude of the rate enhancement. For example, consider the fact that the phosphate group of 2′-CMP is free to rotate in the unbound ligand (with three predominate rotamers). Upon binding to the protein, it is expected that the phosphate group will become fixed in a particular orientation in order to rest at the position of minimum potential with respect to the positively charged histidine residues. For the transition state/intermediate, on the other hand, the pentacoordinated phosphate group is not free to rotate, and no loss of rotational freedom would result upon binding to the enzyme. Therefore, there would be a greater entropy loss of R ln 3 for the binding of 2′-CMP; the Gibbs energy change for the binding of the transition state/intermediate would be expected to be 650 cal/mol more favorable since there would be no such entropy loss. Also, 2′-CMP exists as an equilibrium mixture of syn and anti forms. If only the anti form binds and if the transition state/intermediate is locked into an anti conformation, this would also lead to a more favorable interaction of the latter. From the thermodynamic values of Lavallee & Coulter (1973) for the syn → anti transition of 3′-CMP (using this as a model for 2′-CMP), one can calculate that the Gibbs energy change for the binding of the transition state/intermediate might be 200 cal/mol more favorable than that for the nucleotides for this reason.

Considering the above-mentioned differences in the chemical structure of 2′-CMP and $I^{+,2-}$, it would be reasonable for the latter to be able to bind to RNase A with a Gibbs energy change approximately 0.85 kcal/mol more negative than the former. If ΔG for step 3 is −9.2 kcal/mol, rather than the −8.4 kcal/mol assumed above, then the pK_a of $I^{\pm}$ could be a half a pH unit or so higher than that calculated above. The point is that there may be a number of factors that could lead to an additional interaction between the enzyme and the transition state/intermediate, other than the major interactions that we have included in Scheme IV. Some of these factors could contribute to the enthalpy change for the interaction of the enzyme with the transition state (i.e., there could be enthalpy change and entropy change contributions in addition to those that we have discussed in section B). Therefore, the interactions described by Scheme IV, plus the possible additional factors mentioned above, can account for the magnitude of the rate enhancement for RNase A catalysis provided that the pK_a of the intermediate $I^{+,2-}$ is approximately zero, as we have estimated it to be.

In the above analysis, we have attempted to compare an estimated value of $\Delta G°_I$ (or K_I) to an experimentally calculated value of $\Delta G°_{TS}$ (or K_{TS}). Implicit in this comparison is that $K^{\dagger}_E/K^{\dagger}_{NE}$ is unity in Scheme IV. If, on the other hand, the ratio $K^{\dagger}_E/K^{\dagger}_{NE}$ happened to be much larger or smaller than unity, the above comparison is no longer straightforward. While such possibilities cannot be excluded, nevertheless, Scheme IV and the arguments made above do provide a greater understanding of the energetics of RNase A catalysis

[4] In our analysis above, we have focused on the pK_a of the intermediate $I^{+,2-}$ instead of the transition state since the properties of the latter are generally more difficult to describe. The acidity of the attacking H_2O molecule in the transition state depends on the extent of $H_2O\cdots P$ bond formation (Hegazi et al., 1979). A strategy for determining the pK_a of transition states formed in hydrolysis reactions has been developed by Kurz (1972), but we believe that this method can provide only an upper estimate of the pK_a of a transition state. According to Kurz, such a pK_a can be estimated by comparing the rate constant of a water (solvolysis) reaction with that of a hydroxide reaction. Using this approach and the rate constants reported in the preceding paper (Eftink & Biltonen, 1983b) for the hydrolysis of cCMP, one would estimate a value of ~6 for the pK_a of the transition state. However, the arguments of Kurz are valid only if the transition states for the water and hydroxide reacting are reached at the same point along a reaction coordinate. If either the water or the hydroxide reaction involves a two-step (two transition-state) process, and if the relative heights of the two transition states are different for the water and hydroxide reactions, particularly if the first step (attack) is rate limiting for the water reaction and the second step (elimination) is rate limiting for the hydroxide reaction, the method of Kurz will lead to an overestimate of the pK_a of the transition state.

and enable the rate enhancement of 10^9–10^{10} to be rationalized.

A similar analysis for the transition-state exchange reaction (see Scheme III) can also be made. As listed in Table II, the calculated value of $\Delta G°_{TS}(ex)$ is −14.8 kcal/mol. By considering the exchange of the transition state between imidazole (in solution) and the enzyme's active site (see equation below),

$$\text{Im·TS} + \text{E} \overset{K_{TS(ex)}}{\rightleftharpoons} \text{Im} + \text{E·TS}$$

one focuses on the interactions between the transition state and the enzyme pocket aside from the interaction with His-119. One can again evaluate the magnitude of $\Delta G°_{TS}(ex)$ by using the interaction of 2′-CMP with RNase as a model for the exchange reaction. This accounts for a contribution of −8.4 to −9.2 kcal/mol to $\Delta G°_{TS}(ex)$. Note, however, that the above exchange reaction differs from the simple association reaction of 2′-CMP to RNase in that the catalyst imidazole becomes liberated upon transfer of the transition state to the enzyme. That is, in the binding of 2′-CMP to RNase, there is a loss of translational and rotational entropy for one molecule, which is not the case for the exchange reaction. Because of this factor, the Gibbs energy change for the exchange reaction should be more negative than the $\Delta G°$ for 2′-CMP binding. The absence of a loss of translational entropy [usually estimated to be about 8 cal/(mol·deg) for complex formation] for the exchange reaction can be included in our analysis as an additional contribution of −2.4 kcal/mol to $\Delta G°_{TS}(ex)$. Also, the absence of a loss of rotational entropy for the exchange reaction can be included. This contribution is more difficult to assess but probably would amount to −1 to −3 kcal/mol. Taking these factors into account, we can rationalize a $\Delta G°_{TS}(ex)$ of −12 to −14.5 kcal/mol, which corresponds well with the experimentally calculated value of −14.8 kcal/mol. Thus, again the magnitude of the enzymatic rate enhancement (as compared to the imidazole-catalyzed hydrolysis reaction in this case) can be explained reasonably well in terms of the elementary enzyme–transition-state interactions presented above.

To this point, we have considered the hypothetical upper route of Scheme IV in order to evaluate the energetics and interactions involved in RNase A catalysis. We will conclude by focusing on the sequence of events that take place during the catalytic process (i.e., the lower route in Scheme IV).

In solution, the substrate cCMP is locked in a syn conformation. The substrate binds to the enzyme primarily due to an electrostatic interaction with His-12. Interactions between the pyrimidine ring and the complementary polar groups of the binding site are suboptimal due to the syn conformation of the substrate. The binding of substrate induces some type of change in the conformation of the protein or, more likely, a shift in the distribution of microstates, as evidenced by the negative heat capacity change for K_m. One can speculate that such a conformational change might improve the alignment of certain catalytic side chains with respect to the bound substrate. That this may be the case is suggested by X-ray crystallographic studies which show the position of the His-119 side chain to be more localized in the RNase–3′-CMP complex than the unliganded protein (Richards & Wyckoff, 1971). Other X-ray studies suggest that a change in the conformation and thermal parameters of groups throughout the crystalline protein occurs upon the binding of ligands (Martin, 1978). Once the substrate is bound, the attack of water, assisted by His-119 acting as a general base catalyst, occurs simultaneously with the twisting of the pyrimidine ring to an anti conformation (or a conformation in which the interactions between the pyrimidine ring and the enzyme are greatly improved). The rotation about the glycosidic bond will be coupled to the attack of water since rotation of the bond requires a flexing of the ribose ring in order to avoid nonbonding contacts between atoms of the pyrimidine and ribose rings (Haschmeyer & Rich, 1967; Yathindra & Sundaralingam, 1974). In the substrate, the fused five-membered cyclic phosphate ring forces the ribose ring into a nearly planar, rigid conformation. The ribose ring cannot undergo the flexing needed for rotation about the glycosidic bond. As the O–P–O bond angle in the five-membered ring decreases from ∼109° to ∼90° as water attacks (the bonding about the phosphorus going from a tetrahedral to a trigonal-bipyramidal geometry), the constraints on the ribose ring will be relaxed, allowing for the flexing needed for rotation about the glycosidic bond. Thus, we propose that interactions between the enzyme and the pyrimidine ring are directly coupled to the bond-breaking process. Support for this proposal of a simultaneous twisting and attack comes from studies by Nagyvary & Provenzale (1971) with conformationally restricted nucleotides. They found that O^2,5′-cyclouridine cyclic 2′,3′-phosphate, which has a covalent bridge between the 5′-hydroxyl group and the 2-position of the pyrimidine ring and thus is locked in the syn conformation, is not susceptible to hydrolysis catalyzed by RNase A.

As the transition state is reached, the enzyme must assume a conformation that is somewhat different from the free enzyme (or the distribution of microstates in the enzyme–transition state must be narrower than that for the free enzyme). This again may be a result of the need of the enzyme to adapt its structure, particularly at the active site, in order to be perfectly complementary to the transition state. The similarity of the heat capacity change for the enzyme–substrate and enzyme–transition-state interactions suggests that the induced conformational change may be similar in both cases. Any differences in the conformation of the enzyme between these two states would demand a dynamic participation of the protein during the catalytic step.

Registry No. RNase, 9001-99-4; cyclic 2′,3′-CMP, 633-90-9; 3′-CMP, 84-52-6; 2′-CMP, 85-94-9; L-histidine, 71-00-1.

References

Barnard, P. W. C., & Robertson, R. E. (1961) *Can. J. Chem. 39*, 881–888.

Branch, G. E. K., & Calvin, M. (1941) *The Theory of Organic Chemistry*, Chapter VI, Prentice-Hall, New York.

Cheung, C.-C. S., & Abrash, H. I. (1964) *Biochemistry 3*, 1883–1889.

Crook, E. M., Mathias, A. P., & Rabin, B. R. (1960) *Biochem. J. 74*, 234–238.

del Rosario, E. J., & Hammes, G. G. (1969) *Biochemistry 8*, 1884–1888.

Dixon, M., & Webb, E. C. (1964) *Enzymes, 3rd Ed.* 2, 145–166.

Eftink, M. R., & Biltonen, R. L. (1980a) in *Biological Microcalorimetry* (Breezer, A. E., Ed.) pp 343–412, Academic Press, New York.

Eftink, M. R., & Biltonen, R. L. (1980b) *Biophys. J. 32*, 91–92.

Eftink, M. R., & Biltonen, R. L. (1983a) *Biochemistry* (first of three papers in this issue).

Eftink, M. R., & Biltonen, R. L. (1983b) *Biochemistry* (second of three papers in this issue).

Eftink, M. R., Anusiem, A. C., & Biltonen, R. L. (1983) *Biochemistry 22*, 3884–3896.

Flogel, M., & Biltonen, R. L. (1975a) *Biochemistry 14*, 2603–2609.

Flogel, M., & Biltonen, R. L. (1975b) *Biochemistry 14*, 2610–2615.
Flogel, M., Albert, A., & Biltonen, R. L. (1975) *Biochemistry 14*, 2616–2621.
Haschmeyer, A. E. V., & Rich, A. (1967) *J. Mol. Biol. 27*, 369–384.
Hegazi, M. F., Quinn, D. M., & Schowen, R. L. (1978) in *Transition States of Biochemical Processes* (Gandour, R. D., & Schowen, R. L., Eds.) Chapter 10, Plenum Press, New York.
Herries, D. G., Mathias, A. P., & Rabin, B. R. (1962) *Biochem. J. 85*, 127–134.
Jencks, W. P. (1975) *Adv. Enzymol. Relat. Areas Mol. Biol. 43*, 219–410.
Kitskiakowsky, G. B., & Lumry, R. (1949) *J. Am. Chem. Soc. 71*, 2006–2013.
Kurz, J. L. (1972) *Acc. Chem. Res. 5*, 1–9.
Laidler, K. J. (1955) *Discuss. Faraday Soc. 20*, 83–96.
Laidler, K. J., & Peterman, B. F. (1979) *Methods Enzymol. 63*, 234–257.
Lavallee, D. K., & Coulter, C. L. (1973) *J. Am. Chem. Soc. 95*, 576–581.
Leinhard, G. E. (1973) *Science (Washington, D.C.) 180*, 149–154.
Levy, H. M., Sharon, N., & Koshland, D. (1959) *Proc. Natl. Acad. Sci. U.S.A. 45*, 785–791.
Linden, C. D., Wright, K. L., McConnell, H. M., & Fox, C. F. (1973) *Proc. Natl. Acad. Sci. U.S.A. 70*, 2271–2275.
Lumry, R. (1959) *Enzymes, 1st Ed. 1*, 157–231.
Markley, J. L. (1975) *Biochemistry 14*, 3554–3561.
Martin, P. D. (1978) Ph.D. Dissertation, Wayne State University, Wayne, NE.
Massey, V., Curti, B., & Ganther, H. (1966) *J. Biol. Chem. 241*, 2347–2357.
Matheson, R. R., Jr., & Scheraga, H. A. (1979) *Biochemistry 18*, 2446–2450.
Nagyvary, J., & Provenzale, R. G. (1971) in *Prebiotic and Biochemical Evolution* (Oro, J., & Kimball, A. P., Eds.) p 102, Elsevier/North-Holland, New York.
Patel, D., Canuel, L., & Bovey, F. (1975) *Biopolymers 14*, 987–997.
Raison, J. K. (1973) *J. Bioenerg. 4*, 285–309.
Richards, F. M., & Wyckoff, H. W. (1971) *Enzymes, 3rd Ed. 4*, 647–806.
Tanford, C., Hauenstein, J. D., & Rands, D. G. (1955) *J. Am. Chem. Soc. 77*, 6409–6413.
Thilo, L., Trauple, H., & Overath, P. (1977) *Biochemistry 16*, 1283–1290.
Westheimer, F. H. (1968) *Acc. Chem. Res. 1*, 70–78.
Wolfenden, R. (1972) *Acc. Chem. Res. 5*, 10–18.
Yathindra, N., & Sundaralingam, M. (1974) *Biopolymers 13*, 2061–2076.

Composition and Structure of Zinc-Deficient *Euglena gracilis* Chromatin†

Andrzej J. Stankiewicz, Kenneth H. Falchuk, and Bert L. Vallee*

ABSTRACT: The histone content of zinc-deficient (−Zn) *Euglena gracilis* decreases while, concomitantly, DNA content increases and the transcription rate is reduced markedly [Mazus, B., Falchuk, K. H., & Vallee, B. L. (1983) *Biochemistry* (in press); Falchuk, K. H., Fawcett, D. W., & Vallee, B. L. (1975) *J. Cell Sci. 17*, 57–78]. The effects on major constituents of the genome have been examined by studying the rate and extent of hydrolysis of +Zn and −Zn chromatin by micrococcal nuclease, DNase I, or DNase II. The size of hydrolyzed DNA fragments suggests similarity of the +Zn *E. gracilis* chromatin organization to that of other eukaryotes. The major protein constituent of −Zn chromatin is a polypeptide of less than 3000 daltons whose electrophoretic mobility differs from that of any known histone components of chromatin, the latter described elsewhere (K. H. Falchuk et al., unpublished results). This protein profoundly affects the structure of −Zn chromatin, which is about 10–30-fold more resistant to micrococcal nuclease hydrolysis than +Zn chromatin. Moreover, the resultant DNA fragments [2000 base pairs (bp)], are much larger than those of +Zn cells. Under conditions which hydrolyze +Zn chromatin into DNA fragments smaller than 50 bp, only 50% of −Zn chromatin is digested into fragments <2000 bp, i.e., in the range of those expected for oligonucleosomes. Removal of the low molecular weight protein from −Zn chromatin reverses its enhanced resistance to nucleolysis and results in extensive hydrolysis. Conversely, addition of the low molecular weight protein to +Zn chromatin increases the resistance of this complex to digestion. The results demonstrate the critical importance of zinc to the formation, composition, and structure of normal *E. gracilis* chromatin. The implications to genomic function are discussed.

Zinc is critical to the normal composition and function of the *Euglena gracilis* genome, as is apparent from studies of its deprivation. Zinc deficiency greatly increases the amount of DNA (Wacker, 1962; Falchuk et al., 1975a) while causing the virtual disappearance of the histones (Mazus et al., 1983). Ultimately transcription is repressed (Falchuk et al., 1975a). The characteristics of the protein(s) which replaces (replace) the histones, the effects of their substitution on the structure of chromatin in −Zn cells, and the relationship of such changes to the genomic repression observed in these organisms are all unknown.

The nuclei of +Zn and −Zn *E. gracilis* cells have now been isolated to compare pertinent physical and chemical properties of the respective chromatins. Micrococcal nuclease, DNase I, and DNase II were employed as enzymatic probes. The size of the basic nucleosomal unit of +Zn *E. gracilis* and the histone components of its chromatin are all similar to those of other eukaryotes. The chromatin of −Zn is unlike that found

† From the Center for Biochemical and Biophysical Sciences and Medicine and Department of Medicine, Brigham and Women's Hospital, Harvard Medical School, Boston, Massachusetts 02115. *Received May 2, 1983.* This work was supported, in part, by Grant-in-Aid GM 24989 from the National Institutes of Health of the Department of Health, Education and Welfare.

0006-2960/83/0422-5150$01.50/0